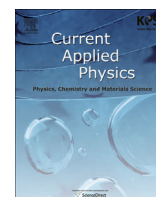




Contents lists available at SciVerse ScienceDirect

## Current Applied Physics

journal homepage: [www.elsevier.com/locate/cap](http://www.elsevier.com/locate/cap)

# Non-volatile memory characteristics of polyimide layers embedded with ZnO nanowires



Jingon Jang<sup>a</sup>, Woanseo Park<sup>a</sup>, Kyungjune Cho<sup>a</sup>, Hyunwook Song<sup>b</sup>, Takhee Lee<sup>a,\*</sup>

<sup>a</sup> Department of Physics and Astronomy, Seoul National University, Gwanak-ro, Gwanak-gu, Seoul 151-742, Republic of Korea

<sup>b</sup> Department of Applied Physics, Kyung Hee University, Giheung-gu, Yongin-si, Gyeonggi-do 446-701, Korea

## ARTICLE INFO

### Article history:

Received 18 December 2012

Accepted 20 March 2013

Available online 2 April 2013

### Keywords:

Organic resistive memory

Non-volatile memory

Write-once-read-many-times

ZnO nanowires

## ABSTRACT

We fabricated  $8 \times 8$  cross-bar array-type organic non-volatile memory devices of polyimide (PI) layers embedded with ZnO nanowires. The ZnO nanowires were synthesized by chemical vapor deposition and deposited into the PI layers by a solution coating process. The devices of PI layer without ZnO nanowires showed an insulating characteristic without exhibiting any memory behavior. The ZnO nanowires acted as carrier trapping sites in the insulating PI layers for our memory devices. The organic memory devices exhibited write-once-read-many-times-type non-volatile memory characteristics with an excellent ON/OFF switching ratio over  $10^6$ , good uniformity in cumulative probability, and stability without serious degradation over  $10^4$  s.

© 2013 Elsevier B.V. All rights reserved.

## 1. Introduction

Organic-based electronics, such as organic photovoltaic cells, field-effect transistors, light-emitting diodes, and memory devices, have been intensively researched over the past decade. Organic materials and devices provide a number of advantages, including simple device structures, large-scale fabrication, good scalability, and flexibility [1–3]. In particular, the viscous inkjet solution-based printability of organic materials is becoming an enabler of future cost-effective electronics technology [4,5]. Among the various device types of organic materials, organic non-volatile resistive memory devices have been widely researched, due to their simple and low-cost fabrication process, good stability, low-power consumption, and multi-stacking capability [6–8]. In organic memory devices, each bi-stable resistive state can be read nondestructively, and there is no need to supply electrical power to maintain a given resistive state, i.e., the memory is non-volatile [9]. Because the properties of organic memory devices primarily depend on the active material itself, a significant amount of research on discovering appropriate materials applicable to organic memory devices has been conducted. Recently, organic memory devices using a chemically producible graphene oxide (GO) as the active layer have been reported [10,11]. From the device structure perspective, the organic memory devices have been manufactured as a single-layer structure, consisting of only one type of organic material; a bi-layer structure, consisting of

two types of organic materials; a tri-layer structure, in which nano-traps for charge carriers are sandwiched between two organic layers; or a spin-cast blend of polymer and nano-traps, in which nano-traps are randomly dispersed in the entire region of the polymer layer [12]. In a tri-layer or composite structure of polymer and nano-traps, finding suitable materials to produce the nano-traps has been the major issue because the organic layers simply act as an insulating host layer. Organic memory devices that use various types of nano-traps materials, such as multilayer graphene, carbon nanotubes, indium phosphide (InP), zinc sulfide (ZnS), cadmium selenide (CdSe), and zinc oxide (ZnO) nano-particles, have recently been reported. The hybrid inorganic/organic nano-composites devices containing nano-traps have exhibited long retention times, indicating excellent device stability [13–17].

In this paper, we fabricated  $8 \times 8$  cross-bar array organic memory devices consisting of polyimide (PI) layers embedded with ZnO nanowires. The ZnO nanowires were synthesized by chemical vapor deposition and deposited within the PI layers by solution-coating. We characterized the fabricated organic memory devices in terms of their switching properties, ON/OFF ratio, cumulative probability, and retention characteristics.

## 2. Experimental details

### 2.1. Device fabrication and characterization

The fabrication process of our organic memory devices is shown in Fig. 1. First, a Si wafer with a 300-nm-thick SiO<sub>2</sub> layer was cleaned

\* Corresponding author. Tel.: +82 2 880 4269; fax: +82 2 884 3002.  
E-mail address: [tlee@snu.ac.kr](mailto:tlee@snu.ac.kr) (T. Lee).

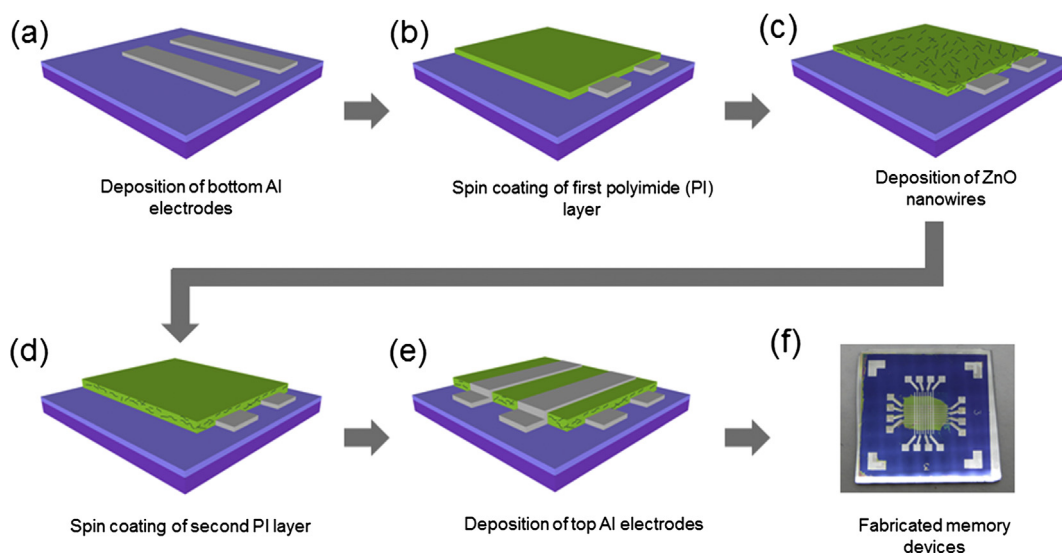


Fig. 1. The fabrication process of our organic memory devices.

using the standard-cleaning process using acetone followed by isopropyl alcohol (IPA) and then de-ionized water in an ultrasonic bath for 10 min. The bottom electrodes (consisting of 50-nm-thick Al) were deposited onto the Si substrate by a thermal evaporator using a 100- $\mu\text{m}$ -line-width shadow mask (Fig. 1(a)). The bottom Al electrodes were exposed to UV-ozone for 10 min to enhance the film uniformity. The polyimide (PI) solution was prepared by dissolving biphenyltetracarboxylic acid dianhydride p-phenylenediamine (BPDA-PPD) in N-methyl-2-pyrrolidone (NMP) with a weight ratio of BPDA-PPD:NMP = 1:3. The prepared PI solution was spin-coated onto the Si substrate at 2000 rpm for 40 s, and the PI-coated Si substrate was subsequently heated on a hot plate at 60 °C for 10 min (Fig. 1(b)). Next, the PI-film/Al-pad structure was

removed from the Si substrate, and the samples were heated at 300 °C for 30 min. After cooling, the IPA solution containing the ZnO nanowires was spin-coated onto the PI-film/Al-pad at 1500 rpm for 10 s, followed by heating at 60 °C for 5 min to evaporate the residual solvent (Fig. 1(c)). After the 10-min UV-ozone cleaning, a second PI layer was spin-coated under the same conditions described above (Fig. 1(d)). Finally, the top electrodes (consisting of 50-nm-thick Al) were deposited by a thermal evaporator with a shadow mask (Fig. 1(e)). By arranging the top and bottom shadow mask lines to cross perpendicularly, 100  $\mu\text{m}$   $\times$  100  $\mu\text{m}$  junctions are produced, each of which define a unit memory cell. A photographic image of completed organic memory devices is shown in Fig. 1(f).

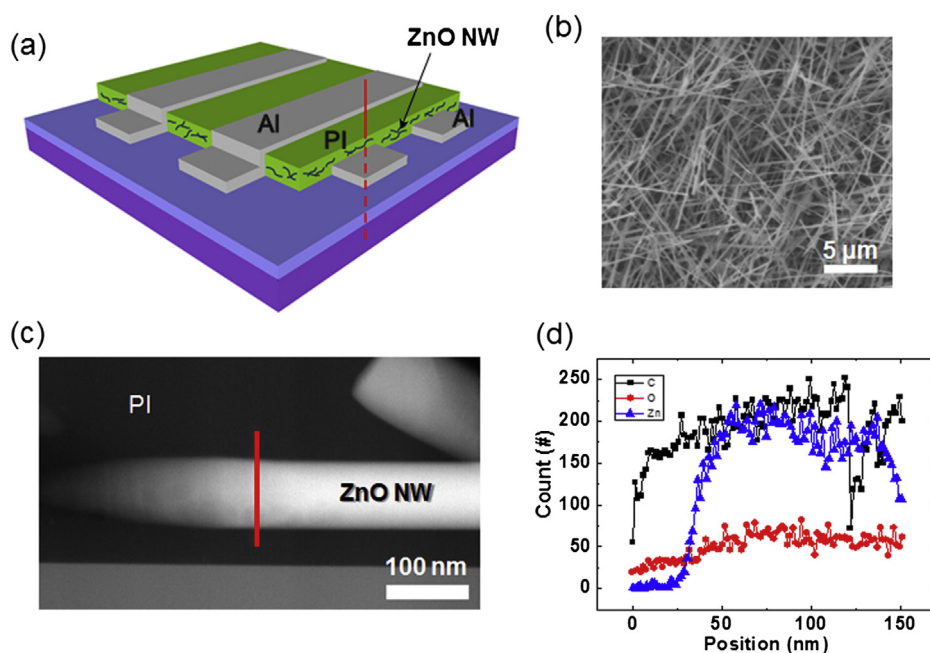


Fig. 2. (a) Schematic of the fabricated organic memory devices. (b) SEM image of the ZnO nanowires grown by chemical vapor deposition. (c) TEM cross-sectional image of a representative organic memory device (across the line in (a)). (d) The compositional profile for the elements of carbon, oxide, and zinc across the line indicated in (c).

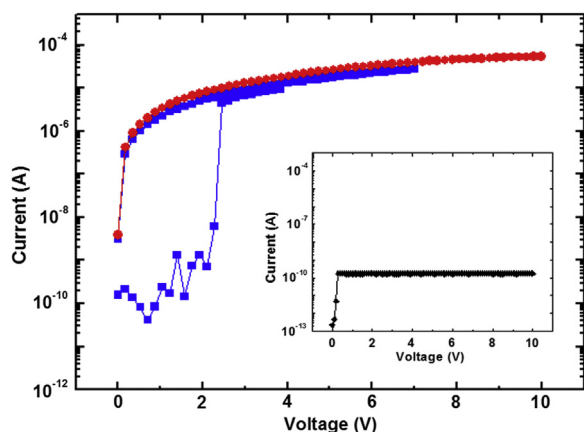


Fig. 3.  $I$ – $V$  characteristics of an organic memory device. The inset shows the data for a device consisting of the polyimide layer without ZnO nanowires.

## 2.2. Synthesis of ZnO nanowires

ZnO nanowires were prepared from ZnO powder and graphite powder using the well-known chemical vapor deposition (CVD) method. A  $c$ -plane sapphire wafer was cleaned by a standard solvent-cleaning process as above, and a 3-nm-thick Au layer was deposited onto the cleaned sapphire wafer by a thermal evaporator. ZnO powder and graphite powder were mixed with an equal mass-ratio uniformly in IPA, and the mixture was dried overnight to vaporize the unnecessary remaining solvent. An alumina boat containing the mixed powder and the Au-coated sapphire was loaded into the center of the quartz tube of the CVD reactor. In the CVD reactor, ZnO nanowires were synthesized on the sapphire substrate under a flow of 50 sccm Ar and 0.2 sccm O<sub>2</sub> for 30 min at  $\sim 920$  °C. After cooling, to disperse the ZnO nanowires, the sapphire substrate coated with ZnO nanowires was soaked with 2 ml of IPA and sonicated for 1 min [18]. Fig. 2(b) shows a scanning electron microscope (SEM) image of the ZnO nanowires grown by the procedure described above. Fig. 2(c) shows a transmission electron microscope (TEM) cross-sectional image of ZnO nanowires in polyimide layers, which was obtained across a line indicated in Fig. 2(a). The elemental profiles along the line profile shown in Fig. 2(d) confirm the presence of ZnO nanowires in the polyimide layers.

## 2.3. Electrical characterization

The electrical measurements were performed using a probe station that was placed in a nitrogen-filled glove box to prevent the

devices from being exposed to the oxygen and moisture present in the ambient atmosphere. The devices were electrically grounded at the bottom electrodes, and the voltage was applied to the top electrodes. The electrical data were obtained with a Keithley-4200-scs-probe station system at room temperature.

## 3. Results and discussion

Fig. 3 shows the representative current versus voltage ( $I$ – $V$ ) characteristics of an organic memory device. We recorded the electrical characteristics of the device in the following sequence. At the beginning of the measurement, voltage was applied from zero to 7 V. After the applied voltage reached 7 V, the voltage was decreased back to zero (blue squares in the web version). Then, the voltage was applied again, but this time over the range from zero to 10 V (red circles in the web version). The initial state of the memory devices was a high-resistive state (OFF state). In the first voltage sweep, when the applied voltage reached  $\sim 2.5$  V, the OFF state of the memory devices was changed to a low-resistive state (ON state). Even if the voltage was decreased back to zero, the ON state remained, indicating the non-volatile character of the memory. When the voltage was applied from zero to 10 V after setting ON state (red line in the web version), the ON state was still maintained, indicating the write-once-read-many-times (WORM) type memory characteristic of the device. This WORM characteristic indicates that the initial OFF state of the organic memory device can be switched to the ON state but that the device cannot be switched back to the OFF state. A memory device that is switchable between the ON and OFF states (called rewritable switching) is preferred, but the WORM-type organic memory devices are also useful, as long as the ON and OFF states can be stably maintained in a manner similar to that in CD-ROM type memory.

Our memory devices consisting of PI embedded with ZnO nanowires exhibited WORM-type non-volatile memory with a high ON/OFF ratio (Fig. 3). If the ZnO nanowires were not embedded into the PI layers, those organic devices with only the PI layer did not exhibit any memory properties. Instead, they exhibited electrical insulating behavior, thus confirming that the ZnO nanowires played the role of the material that produced nano-traps in our organic memory devices, whereas the polyimide layer acted only as an insulating layer.

The observed memory switching characteristics can be explained by the charging effect of the ZnO nanowires embedded between the insulating polyimide layers. It is well known that the work function of Al and the ZnO nanowires is  $\sim 4.3$  eV and  $\sim 5.3$  eV, respectively [19,20]. When the voltage is applied, the carriers from

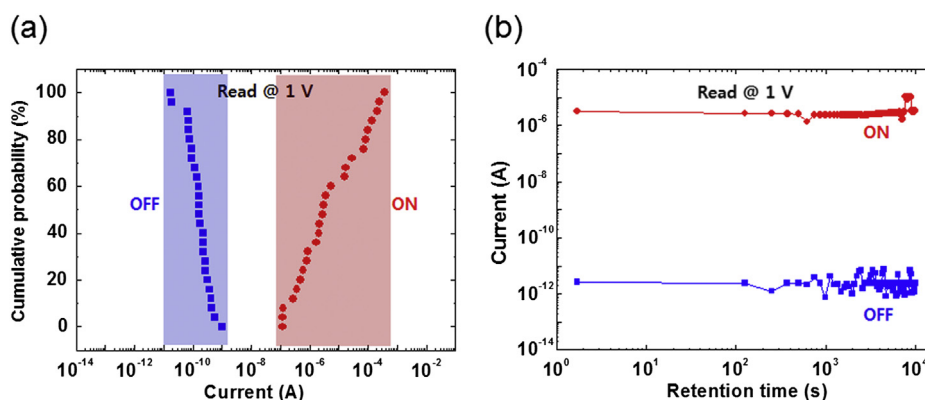


Fig. 4. (a) The cumulative probability and (b) the retention characteristics of our organic memory devices.

the Al electrode are injected into the insulating polyimide layer and ZnO nanowires. Here, because of the work function difference between the Al and the ZnO nanowires, the injected carriers are trapped in the ZnO nanowires, resulting in charge accumulation. With sufficient applied voltage, the trapped carriers can penetrate into the other polyimide layer, and the accumulated internal charge generates a local electric field, which ultimately affects the switching behavior, i.e., a filamentary path is formed. This charging effect observed in the organic memory devices has been reported previously for many types of nano-trap materials, including ZnO nano-crystals [15,16,21].

In addition to the switching characteristics, organic memory devices should be characterized in terms of memory performance, such as uniformity in the cumulative probability and retention characteristics. Fig. 4(a) shows the cumulative probability of the ON and OFF resistive states in the memory devices that were characterized. Although the ON state was relatively wide, each state was well separated by at least  $10^2$  times the current level, which confirmed that reliable memory operation is possible. Fig. 4(b) shows the retention times of our organic memory devices. Each state was maintained over  $10^4$  s at 1 V (reading voltage) without serious degradation, indicating the bi-stability of the devices.

#### 4. Conclusions

In summary, we investigated  $8 \times 8$  cross-bar array-type organic memory devices consisting of polyimide layers embedded with ZnO nanowires. The ZnO nanowires, synthesized by chemical vapor deposition, were deposited into the polyimide layers by solution spin-coating, and they were used as carrier trapping sites in the insulating polyimide layers. The organic memory devices exhibited WORM-type memory characteristics with an excellent ON/OFF switching ratio of over  $10^6$  and a good retention property of over  $10^4$  s. Although there is some improvement required to improve the density of the ZnO nanowires embedded in the polyimide layers, the solution-coating method used to disperse the ZnO nanowires is a convenient tool to form the active layer in a composite structure in organic memory devices.

#### Acknowledgments

This work was supported by the National Creative Research Laboratory program (Grant No. 2012026372) and the National Core Research Center (Grant No. R15-2008-006-03002-0) from the Korean Ministry of Education, Science, and Technology, and RIAM (Research Institute of Advanced Materials) of Seoul National University.

#### References

- [1] J.C. Scott, L.D. Bozano, Nonvolatile memory elements based on organic materials, *Adv. Mater.* 19 (2007) 1452–1463.
- [2] H.E. Katz, J. Huang, Thin-film organic electronic devices, *Annu. Rev. Mater. Res.* 39 (2009) 71–92.
- [3] Q. Ling, D. Liaw, C. Zhu, D. Chan, E. Kang, K. Neoh, Polymer electronic memories: materials, devices and mechanisms, *Prog. Polym. Sci.* 33 (2008) 917–978.
- [4] M. Singh, H.M. Haverinen, P. Dhagat, G.E. Jabbour, Inkjet printing – process and its applications, *Adv. Mater.* 22 (2010) 673–685.
- [5] T. Aernouts, P. Vanlaeke, W. Geens, J. Poortmans, P. Heremans, S. Borghs, R. Mertens, R. Andriessen, L. Leenders, Printable anodes for flexible organic solar cell modules, *Thin Solid Films* 451–452 (2004) 22–25.
- [6] B. Cho, S. Song, Y. Ji, T. Kim, T. Lee, Organic resistive memory devices: performance enhancement, integration, and advanced architectures, *Adv. Funct. Mater.* 21 (2011) 2806–2829.
- [7] M.A. Khan, U.S. Bhansali, H.N. Alshareef, High-performance non-volatile organic ferroelectric memory on banknotes, *Adv. Mater.* 24 (2012) 2165–2170.
- [8] K. Yook, J. Lee, Transparent organic bistable memory devices using a low resistance transparent electrode, *Thin Solid Films* 517 (2009) 5573–5575.
- [9] Y. Ji, B. Cho, S. Song, T. Kim, M. Choe, Y. Kahng, T. Lee, Stable switching characteristics of organic nonvolatile memory on a bent flexible substrate, *Adv. Mater.* 22 (2010) 3071–3075.
- [10] C.L. He, F. Zhuge, X.F. Zhou, M. Li, G.C. Zhou, Y.W. Liu, J.Z. Wang, B. Chen, W.J. Su, Z.P. Liu, Y.H. Wu, P. Cui, R.W. Li, Nonvolatile resistive switching in graphene oxide thin films, *Appl. Phys. Lett.* 95 (2009) 232101.
- [11] H. Jeong, J.Y. Kim, J.W. Kim, J. Hwang, J.E. Kim, J. Lee, T. Yoon, B. Cho, S. Kim, R.S. Ruoff, S. Choi, Graphene oxide thin films for flexible nonvolatile memory applications, *Nano Lett.* 10 (2010) 4381–4386.
- [12] T. Lee, Y. Chen, Organic resistive nonvolatile memory materials, *MRS Bull.* 37 (2012) 144–149.
- [13] F. Li, D. Son, B. Kim, T. Kim, Nonvolatile electrical bistability and operating mechanism of memory devices based on CdSe/ZnS nanoparticle/polymer hybrid composites, *Appl. Phys. Lett.* 93 (2008) 021913.
- [14] J. Ham, D. Oh, S. Cho, J. Jung, T. Kim, E. Ryu, S. Kim, Carrier transport mechanisms of nonvolatile write-once-read-many-times memory devices with InP–ZnS core-shell nanoparticles embedded in a polymethyl methacrylate layer, *Appl. Phys. Lett.* 94 (2009) 112101.
- [15] K. Park, J. Jung, F. Li, D. Son, T. Kim, Carrier transport mechanisms of nonvolatile memory devices based on nanocomposites consisting of ZnO nanoparticles with polymethylmethacrylate nanocomposites sandwiched between two  $C_{60}$  layers, *Appl. Phys. Lett.* 93 (2008) 132104.
- [16] Y. Ji, M. Choe, B. Cho, S. Song, J. Yoon, H. Ko, T. Lee, Organic nonvolatile memory devices with charge trapping multilayer graphene film, *Nanotechnology* 23 (2012) 105202.
- [17] S. Hwang, J. Lee, S.J. Kim, J. Park, H. Park, C. Ahn, K. Lee, T. Lee, S.O. Kim, Flexible multilevel resistive memory with controlled charge trap B- and N-doped carbon nanotubes, *Nano Lett.* 12 (2012) 2217–2221.
- [18] G. Jo, W. Hong, J. Sohn, M. Jo, J. Shin, M.E. Welland, H. Hwang, K.E. Geckeler, T. Lee, Hybrid complementary logic circuits of one-dimensional nanomaterials with adjustment of operation voltage, *Adv. Mater.* 21 (2009) 2156–2160.
- [19] C. Lee, T. Lee, S. Lyu, Y. Zhang, H. Ruh, H. Lee, Field emission from well-aligned zinc oxide nanowires grown at low temperature, *Appl. Phys. Lett.* 81 (2002) 3648.
- [20] J. Hwang, D. Lee, J. Kim, T. Han, B. Kim, M. Park, K. No, S. Kim, Vertical ZnO nanowires/graphene hybrids for transparent and flexible field emission, *J. Mater. Chem.* 21 (2011) 3432–3437.
- [21] J. Jung, J. Jin, I. Lee, T. Kim, H. Roh, Y. Kim, Memory effect of ZnO nanocrystals embedded in an insulating polyimide layer, *Appl. Phys. Lett.* 88 (2006) 112107.